Science of Sintering, **49** (2017) 197-205

doi: https://doi.org/10.2298/SOS1702197S

UDK 552.52, 661.872.2

Iron (III) Oxide Fabrication From Natural Clay With Reference to Phase Transformation γ- → α- Fe_2O_3

Aleksandra Šaponjić[1*)], Đorđe Šaponjić[1], Violeta Nikolić[1], Maja Milošević[2], Milena Marinović-Cincović[1], Stanislav Gyoshev[3], Marina Vuković[4], Maja Kokunešoski[1]

[1] University of Belgrade - Vinča Institute of Nuclear Sciences, Belgrade, Serbia
[2]University of Belgrade - Faculty of Mining and Geology, Belgrade, Serbia
[3]Institute of Information and Communication Technologies, Bulgarian Academy of Sciences, Sofia, Bulgaria
[4]University of Belgrade - Institute for Multidisciplinary Research, Belgrade, Serbia

Abstract:

Amorphous iron (III) oxide was obtained from clay, using ammonium hydroxide as a precipitating agent. Influence of freeze drying under vacuum, as a drying method, on particle size, chemical composition, and crystallinity of obtained iron (III) oxide powder was investigated. After freeze drying, precipitate was annealed in air at 500 °C and 900 °C. X-ray diffraction, particle size analysis, scanning electron microscopy, energy dispersive spectrometry, Fourier transform infrared spectroscopy, thermogravimetric and differential thermal analysis were used to characterize obtained iron (III) oxide powder. All of three powders obtained by freeze drying and annealing, have low crystallinity and particles with irregular layered shape. Narrow particle size distribution was given by an average diameter value of around 50 μm for all observed powders. Iron-bearing materials like α-Fe_2O_3 and γ-Fe_2O_3 are obtained. Differential thermal analysis curve of obtained samples showed endothermic reaction at 620 °C which could be ascribed to phase transition from cubic form γ- → α- Fe_2O_3. Thermal transformations of iron (III) oxide, obtained from clay as a natural source, is suitable to explore in the framework of materials chemistry, and opens the possibility to synthesize materials based on Fe_2O_3 with specific magnetic behavior.

Keywords: *Clay; Iron (III) oxide; Precipitation; Freeze drying; TG-DTA.*

1. Introduction

European countries increasingly apply exploitation of accompanying minerals in coal mine deposits such as clay, sand, gravel, coal gangue, diatomaceous earth, fly ash, etc. Iron (III) oxide is one of the ingredients of clay. Thermal transformations of iron bearing materials from minerals in oxidizing atmosphere are processes investigated in various fields of chemistry, mineralogy and materials science: goethite [1-7], akaganeite [8], lepidocrocite [9-10], siderite [11], pyrite [12-16], pyrrhotite [15-17], almandine [18], biotite [19-20], phlogopite [20], vermiculite [20], illite [21], or ilmenite [22-23]. The common point of these processes is formation of different iron oxides during conversion and/or oxidation of

*) **Corresponding author**: saponjic@gmail.com

products. Iron (III) oxide is one of the most used metal oxides. Micrometre-sized particles of iron (III) oxide, with narrow size distribution, have various applications in many scientific and industrial fields. Iron oxides are used for production of iron and steel, also as pigments, catalysts, sensors, adsorbents, materials for magnetic data recording, etc. [24-33]. Its most frequent polymorphs forms are hematite (α- Fe_2O_3) and maghemite (γ- Fe_2O_3).

Near Belgrade there is a huge basin of coal (surface coal mine Kolubara, Serbia) mixed with layers of clay. During exploitation of coal a huge amount of clay is deposited as mullock. This work describes a possibility to obtain iron (III) oxide from clayey material as a raw material by co-precipitation method, and then freeze dried under vacuum. This method does not require any specialized facilities.

The material made of mesoporous material, like SBA-15 and amorphous Fe_2O_3, opens possibility to obtain materials of specific magnetic or catalytic behavior, which will be a possible subject of future research. Magnetic behavior of the obtained materials based on Fe_2O_3 will be also studied, first.

2. Experimental

2.1. Procedure

Clay as a source of iron (III) oxide was purified using thermal and chemical treatments before processing. Organic impurities have been removed from the material by heat treatment (600 °C, 2 h) in air. Clay was treated in an acidic medium of HCl (aqueous solution of 0.5 M HCl, p.a. 37 %, BDH Prolabo) (wt.% 1:10) in order to leach iron. Suspension was stirred at 60 ^oC for 6 h, and afterwards at room temperature for 6 day south of mixing. Iron (III) oxide, was obtained from filtrate by precipitation method using ammonium hydroxide as a precipitation agent followed by decanting liquid phase. Obtained precipitate was washed several times with distilled water until the neutral reaction. Powder was prepared by freeze drying using Modulyo Freeze Dryer System Edwards, England, consisting of freeze dryer unit at High Vacuum Pump E 2 M 8 Edwards. The precipitate was pre-frozen at -30 °C and then freeze dried for 24h. Vacuum during 24 h long freeze drying was around 4 mbar. The powders were annealed in air (1 ^oC/min) at 500 ^oC and at 900 ^oC, for 6 h.

2.2. Characterizations

Sandy clay from surface coal mine Kolubara, Serbia was used as a raw material. Chemical compositions of starting and thermally and chemically treated clays, obtained by inductively coupled plasma (ICP) spectrometry (Spectro-Flame, Spectro-Analytical Instruments), are listed in Tab. I [38].

Tab. I Chemical composition (percentage weight: wt%) of the starting and thermally and chemically treated clay materials [38].

Element	Al_2O_3	Fe_2O_3	TiO_2	MgO	CaO	Na_2O	K_2O	SiO_2
As-receved clay, wt.%	6.05	2.06	0.48	0.35	0.18	1.05	1.76	88
Thermally and chemically treated clay, wt.%	5.10	0.96	0.52	0.25	0.21	1.21	1.53	90

Samples containing iron oxide particles were characterized at room temperature by X-ray powder diffraction (XRD) by using Philips PW-1050 diffractometer with Ni-filtered Cu-Kα radiation (1.54178 Å). The range of 2°-80° 2θ was used in a continuous scan mode with a scanning step size of 0.05° at scan rate of 1 °/min. The same analysis was used to characterize clay fraction smaller than 63 μm, corresponding to 37.82 % of the original mass of clay sample with (2–60° 2θ, continuous scan mode with a scanning step size of 0.02° at a scan rate of 2 °/min). XRD patterns of the as-received clay and treated clay, are shown in Fig. 1. Quartz (PDF No. 33-1161) is the major phase in starting and treated clays. The X-ray diffractogram (inset in Fig. 1) of oriented sample of the as-received clay showed diffraction peaks that indicate presence of some clay minerals: kaolinite, 7.291 Å (PDF:No. 89-6538), mica/illite, 10.054 Å (PDF: No. 88-2198) and 2:1 clay, probably montmorillonite 6.16 Å (PDF: No. 29-1498) [35]. There are some differences between the peak intensities of both, as-received and treated clay sample.

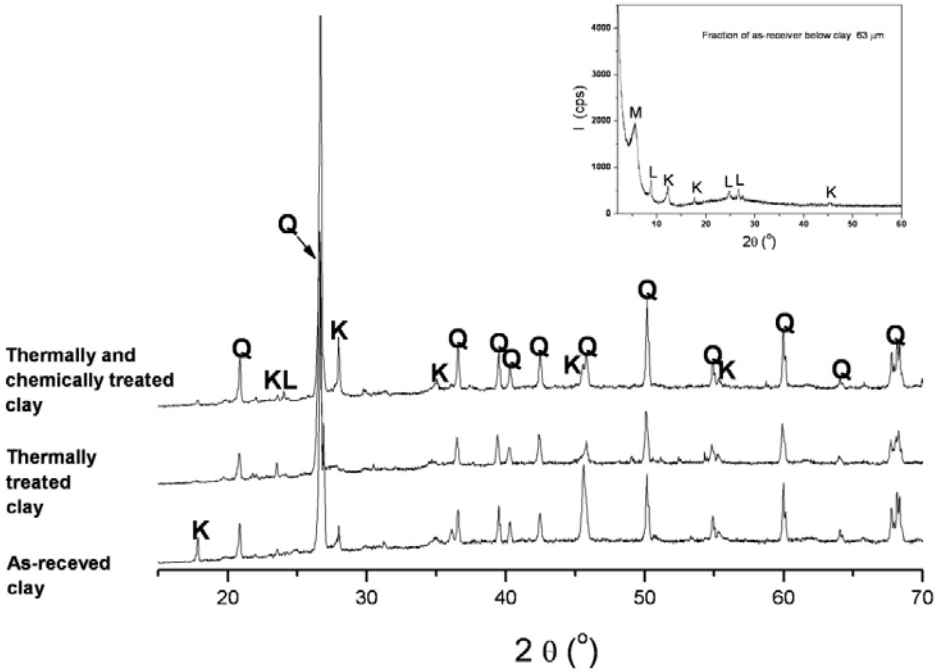

Fig. 1. XRD patterns of the samples: as-received and treated clays: Q quartz, K kaolinite, L mica/illite, M montmorillonite [35].

An ANALYSETTE 22 Micro Tec plus was employed to determine particle size of iron (III) oxide powder. Microstructure analysis is performed by scanning electron microscope (SEM, VEGA TS 5130 MM, Tescan). X-ray microanalysis (EDS) was carried out with INCA PentaFET-x3, Oxford Instruments. Functional groups of iron (III) oxidewere studied by using Fourier transform infrared (FTIR) spectroscopy. Infrared spectrum of the powder sample was recorded at ambient conditions between 4000–400 cm^{-1} (mid-IR region) with a Nicolet IS 50 FTIR. Thermal stability of samples was investigated by simultaneous non-isothermal thermo-gravimetric analysis (TG) by using a SETARAM SETSYS Evolution 1750 instrument. The measurements were conducted at a heating rate of 10 °C/min in air atmosphere (flow rate was 16 cm^3/min) in the temperature range of 30–1000 °C. Furnace A.D.A.M.E.L equipped with Pt-Pt/Rh thermocouples, together with the digital data acquisition computer system, has been used to obtain differential thermal analysis (DTA).

3. Results and Discussion

3.1. X-ray diffraction (XRD)

Chemical composition of the as-received and treated clay is mainly composed of SiO_2 and Al_2O_3, also oxides like Fe_2O_3, Na_2O and K_2O are present (Tab. I) [8]. Fig. 2 shows XRD patterns of the freeze dried powder and powders annealed at 500 °C and at 900 °C with line broadening caused by reduced size of crystallites and low crystallinity. It was hard to identify the exact positions of diffraction peaks.

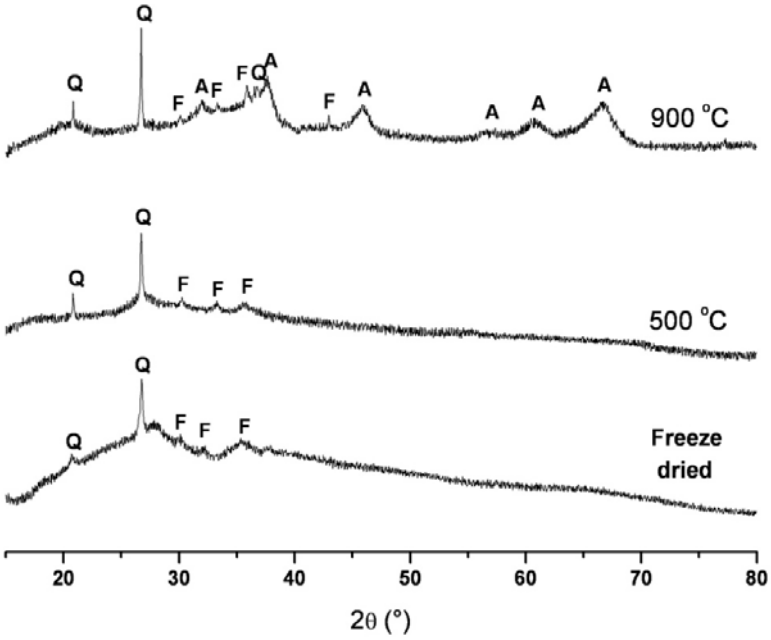

Fig. 2. XRD patterns of freeze dried sample and samples, anniled at 500 °C/900 °C: Q-quartz (SiO_2), F- α-Fe_2O_3, A-σ-Al_2O_3.

The XRD pattern of samples annealed at 500 °C, exhibited a remarkable broadening in 2θ region from 20-33° which is associated with the presence of amorphous silica. In the case of sample annealed at 900 °C, quartz SiO_2 (PDF: No. 33-1161) and σ- Al_2O_3 (PDF: No. 88-1609) are the main reaction products, in addition toγ- and α-Fe_2O_3(PDF: No. 89-8104, PDF: No. 89-5892). According to Park et al. [36] and Zhong and Zhang[37] the intermediate crystalline phase, such as α- or γ- Fe_2O_3, are often derived in the sol-gel and co-precipitate precursors when they are calcined, as in our case. There are some differences in peak intensities between the samples sintered at different temperatures (500 °C and 900 °C (Fig. 2)). These observations are in good agreement with the results obtained by TG/DTA analyses (Part 3.5., Fig. 6.).

3.2. Analysis of Particle Size

The specimen annealed at 900 °C (Fig. 3a) has slightly narrowed particle size distribution in comparison with powders obtained by freeze drying and annealed at 500 °C. Particle size distribution was given by an average diameter value of 47.9 μm for the powder obtained by the freeze drying method. For samples annealed at 500 °C and 900 °C the average particle diameters are 53.9 and 49.8 μm, respectively. All of these observations are in good agreement with results obtained by the SEM analyses (Fig. 3b).

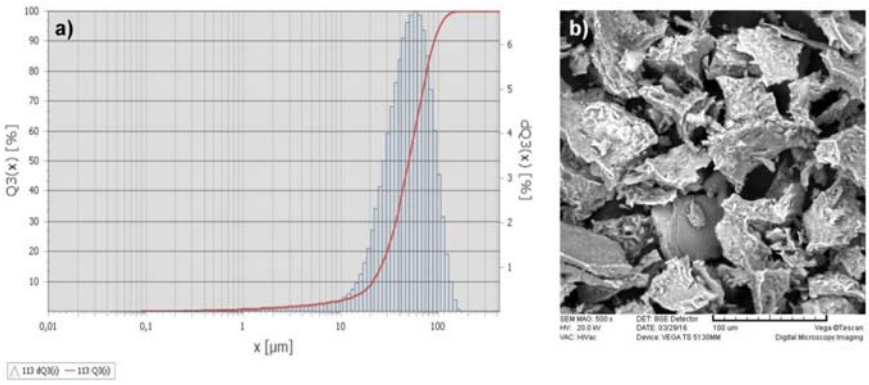

Fig. 3. Powder anealled at 900 °C: particle size distribution curve (a) and SEM image (b).

3.3. Scanning electron microscope and energy dispersive spectrometry (SEM/EDS)

Inherent layered structure of the clay seems to be retained in both samples, obtained at 500 °C and 900 °C. According to Zboril et al. [34] in some cases, Fe_2O_3 particles showed tendency to maintain structural or morphological features of the original compound as in our case. Energy dispersive spectrometry (EDS) analysis showed the obvious signals for Fe and O elements (Fig. 4). Other elements were detected as well; owing to the fact that iron was precipitated from natural clay (Tab. I) [38] and Cl used in the chemical treatment of clay. This is probably due to the fact that the fine fraction of clay is likely to lag behind in the preparation process, which is confirmed by XRD analysis (Fig. 2).

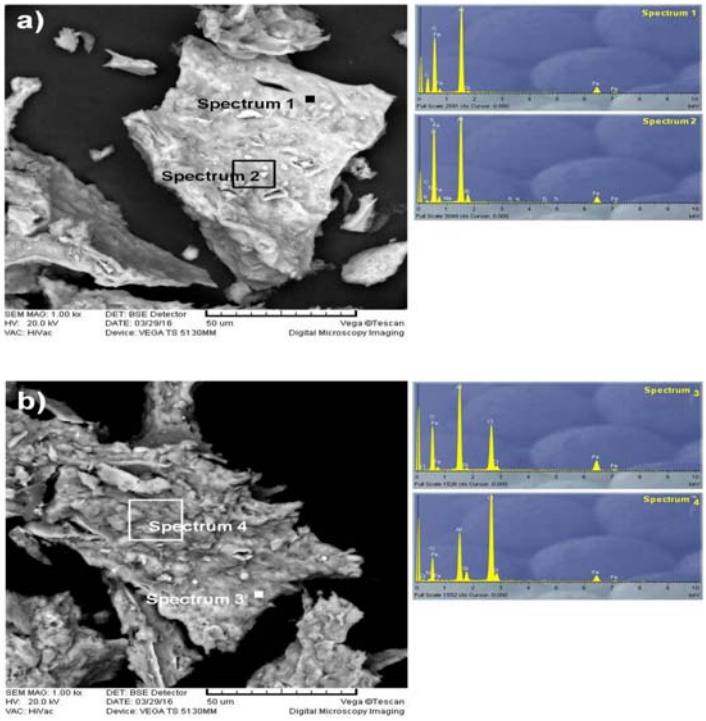

Fig. 4. SEM micrographs of powders annealed at 500 °C (a) and 900 °C (b) with their EDS spectras.

3.4. Fourier transformation infrared (FTIR) spectroscopy

Measurements were performed on freeze dried sample, and samples annealed at 500 °C, and at 900 °C (Fig. 5).As one can notice from FTIR, spectra of the freeze dried sample and sample annealed at 500 °C are rather similar. Bands in high wave number region, as well as bend at 1630 cm^{-1}, are attributed to -OH groups vibration of interlayer water molecules present in the clay [39]. Vibrations at 1398 cm^{-1} and 1040 cm^{-1} indicate appearance of SiO_2 [40,41], while band at 850 cm^{-1} is attributed to Al-Mg-OH band vibration [39]. The sample annealed at 900 °C showed absence of characteristic bands (in accordance with XRD results) pointing to thermal degradation of the clay at higher temperatures. Band at 1086 cm^{-1} is ascribed to Si-0-Si symmetric stretching vibration [42]. Fig. 5 shows enlarged low wave number region which is characteristic for Fe-O vibrations. As ICP spectrometry showed a significantly lower content of iron (III) oxide compared to SiO_2. The bands originated from iron oxides are weak and broad (Tab. I) [38].

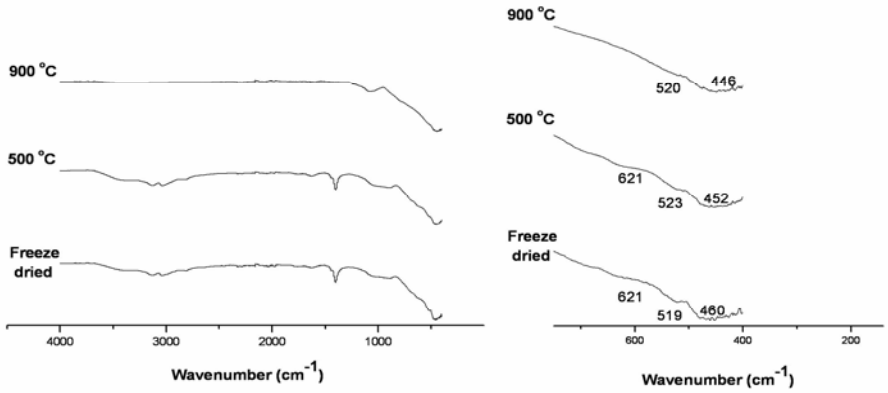

Fig. 5. FT-IR spectra of the freeze dried sample and samples annealed at 500 °C and 900 °C.

Shoulder at 621 cm^{-1} in freeze dried sample and sample annealed at 500 °C, attributed to the Fe-O bond, appeared as a consequence of decrease in crystal symmetry, characteristic for γ- Fe_2O_3 phase [43]. Spectrum of the sample annealed at 900 °C presented two bands at similar positions as in the spectra of the sample annealed at 500 °C. As XRD investigation confirmed the absence of clay at 900 °C. The observed bands in this region are attributed to Fe-O bands vibration. Band at 428 cm^{-1} pointed at the presence of Fe-O vibration, while the band at 540 cm^{-1} is characteristic for α- Fe_2O_3 phase [40]. Absence of band at 621 cm^{-1} (characteristic for γ-Fe_2O_3 phase) and, simultaneously, appearance of the band at 520 cm^{-1}, could be indicative of phase transformation γ- → α- Fe_2O_3 phase. These observations are also confirmed by TG/DTA measurements (Part 3.5., Fig. 6).

3.5. Thermo-gravimetric analysis and differential thermal analysis (TG/DTA)

TG/DTA curves of the samples obtained by freeze drying and annealed at 500 °C are shown in Fig. 6. TG curve of sample obtained by freeze drying shows two-stage weight loss at the temperature ranges about of 30–150 °C and 150–540 °C (Fig. 6a). Weight loss at 30–150 °C can be attributed to evaporation of free adsorbed water is evidenced from an endothermic peak at 110 °C in the DTA curve (Fig. 6b). A gradual weight loss from 150 °C to 290 °C (Fig. 6a) is due to dehydroxylation of chemically bonded water. Two broad exothermic peaks in the DTA curve around 190 and 285 °C, also emphasize the same (Fig. 6b). These two peaks are distinctive of iron, iron oxy hydroxides and oxides. The Process of dehydroxylation of the chemically bonded water ends at around 400 °C with formation of γ-

Fe_2O_3 phase (maghemite) [44-46]. Exothermic reaction, around 400 °C could probably be ascribed to further rearrangement of the crystal structure to cubic form of γ-Fe_2O_3 (maghemite). The endothermic reaction at 620 °C could be ascribed to further rearrangement of crystal structure to phase transition from cubic form γ- to α- Fe_2O_3 (trigonal). The temperature range of the endothermic peaks at 720 °C and 860 °C seems to correspond well with literature data [44-46]. Peak from the exothermic reaction at 400 °C has lower intensity in the sample obtained at 500 °C relative to the sample obtained by freeze drying, thus indicating that the reaction of rearrangement of the crystal lattice was occurred at lower temperatures. Also, there are no endothermic reactions at 720 °C and 860 °C in the sample annealed at 500 °C. This means that the sample has already undergone thermal treatment which can be inferred from a much smaller amount of moisture and constitutional water (Fig. 6b) [44-46]. These results are in accordance with the FTIR investigation.

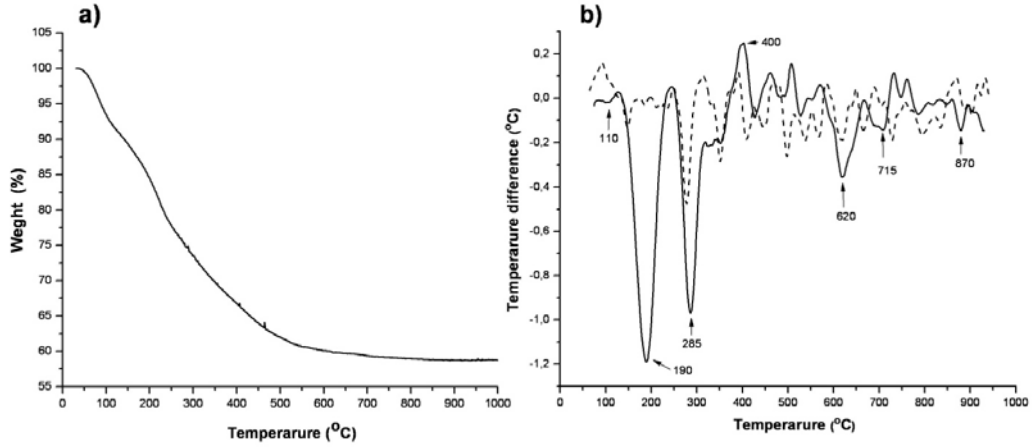

Fig. 6. TG a) and DTA b) curves of the samples obtained by (—) freeze drying and (---) annealing at 500 °C.

4. Conclusions

Iron oxides were obtained from clay as a raw material by co-precipitation as a simple and inexpensive method. Benefit of this method is that it does not require any specialized facilities. Synthesized particles of iron oxides by the freeze drying and annealed at 500 °C and 900 °C have size around 50 μm. The obtained Fe_2O_3 particles could be used as catalysts or catalyst support.

Acknowledgments

The authors thank Ministry of Education, Science and Technological Development of the Republic of Serbia for support of this investigation through projects III-45012, OI-172045, III-45015, OI-176010, OI-172056 and III-45007. The authors are grateful to Vojislav Aranđelović and Branko Matović for help and support.

5. References

1. M. Pelino, L. Toro, M. Petroni, J. Mater. Sci., 24 (1989) 409.
2. M. P. Pomies, M. Menu, C. Vignaud, J. Eur. Ceram. Soc., 19 (1999) 1605.

3. M. J. Dekkers, Geophys. J. Int., 103 (1990) 233.
4. A. F. Gualtieri, P. Venturelli, Am. Mineral., 84 (1999) 895.
5. M. P. Pomies, G. Morin, C. Vignaud, Eur. J. Solid State Inorg. Chem., 35 (1998) 9.
6. M. Rosler, E. Held, H. Hofmeister, J. Magn. Magn. Mater., 120 (1993) 48.
7. L. Diamandescu, D. Mihaila-Tarabasanu, M. Felder, Mater. Lett., 17 (1993) 309.
8. M. R. Cornell, R. Givanoli, Clay. Clay Miner., 39 (1991) 144.
9. P. M. A. de Bakker, L. H. Bowen, R. J. Pollard, J. Phys. Chem. Miner., 18 (1991) 131.
10. J. M. Criado, G. S. Chopra, C. Real, Chem. Mater., 11(1999) 1128.
11. S. B. Jagtap, A. R. Pande, A. N. Gokarn, Int. J. Miner. Process, 36 (1992) 113.
12. Y. Hong, B. Fegley, Jr. Ber. Bunsen-Ges. Phys. Chem., 101 (1997) 1870**.**
13. P. P. Kirilov, I. N. Gruncharov, Y. G. Pelovski, Thermochim. Acta, 244 (1994) 79.
14. V. A. Luganov, V. I. Shabalin, Can. Metall. Quart., 33 (1994) 169.
15. J. G. Dunn, L. C. Mackey, J. Therm. Anal., 39 (1993) 1255.
16. F. Paulik, M. Arnold, J. Therm. Anal, 39 (1993) 1079.
17. H. F. Steger, Chem. Geol., 35 (1982) 281.
18. M. Mašláň, Z. Šindelář, P. Martinec, M. Chmielová, A. L. Kholmetskii, Czech. J. Phys., 47 (1997) 571.
19. C. S. Hoog, R. E. Meads, Mineral. Magn., 40 (1975) 89.
20. R. P. Tripathi, U. Chendra, R. Chandra, S. Lokanathan, J. Inorg. Nucl. Chem. 40 (1978) 1293.
21. U. Wagner, W. Knorr, A. Forster, E. Murad, R. Salazar, F. E. Wagner, Hyperfine Interact., 41 (1988) 855.
22. M. Manrique, T. Figueira, P. R. Taylor, Astrophys. Space Sci., 256 (1997) 499.
23. A. R. Briggs, A. Sacco, Jr. Metall. Trans. A-Phys. Metall. Mater. Sci., 24 (1993) 1257.
24. R. M. Cornel, U. Schwertmann, The Iron Oxides. Structure, Properties, Reactions and Uses, VCH, Weinheim, 1996.
25. T. R. Prasad, K.V. K. Rao, J. S. Murty, J. S. Met., Mater. Process, 9 (1997) 9.
26. G. P. Vissokov, P. S. Pirgov, J. Mater. Sci., 31 (1996) 4007.
27. J. Bohacek, J. Subrt, T. J. Hanslik, T. J. Mater. Sci., 28 (1993) 2827.
28. Montreal Society for Coatings Technology. J. Coat. Technol., 61 (1989) 73.
29. M. Matsuoka, Y. Nakatani, H. Ohido, Nat. Tech. Rep., 24 (1978) 461.
30. R. D. McMichael, R. D. Shull, L. J. Swartzendruber, L. H. Bennett, J. Magn. Magn. Mater., 111 (1992) 29.
31. L. Günther, Phys. World 3 (1990) 28.
32. G. Shoün, U. Simon, Colloid Polym. Sci., 273 (1995) 101.
33. L. Nixon, C. A. Koval, R. D. Noble, Chem. Mater., 4 (1992) 117.
34. R. Zboril, M. Mashlan, D. Petridis, Chem. Mater., 14 (2002) 969.
35. M. Kokunešoski, A. Šaponjić, M. Stanković, J. Majstorović, A. Egelja, S. Ilića, B. Matović, Ceram. Int., 42 (2016) 6383.
36. J. Y. Park, S. G. Oh and B. H. Ha, Korean J. Chem. Eng., 18 (2001) 215.
37. W. D. Zhong and N. Zhang, J. Magn. Magn. Mater., 168 (1997) 196.
38. M. Kokunešoski, A. Šaponjić, V. Maksimović, M. Stanković, M. Pavlović, J. Pantić, J. Majstorović, Ceram. Int., 40 (2014) 14191.
39. T. Novaković, Lj. Rozić, S. Petrović, A. Rosić, Chem. Eng. J., 137 (2008) 436.
40. A. E. Panasenko, I. A. Tkachenko, L. A. Zemnukhova, I. V. Shchetinin, N.A. Didenko, J. Magn. Magn. Mater., 405 (2016) 66.
41. F. Rubio, J. Rubio, J. L. Oteo, Spectrosc. Lett., 31 (1998) 199.
42. J. Osswald, K. T. Fehr, J. Mater. Sci., 41 (2006) 1335.
43. M. Gotić, G. Koščec, S. Musić, J. Mol. Struct., 924–926 (2009) 347.
44. Y. Ichiyanagi, Y. Kimishima, J. Therm. Anal. Cal., 69 (2002) 912.

45. S. Bharathi, D. Nataraj, D. Mangalaraj, Y. Masuda, K. Senthil, K. Yong, J. Phys. D: Appl. Phys., 43 (2010) 1.
46. X. Wang, X. Chen, L. Gao, H. Zheng, M. Ji, C. Tang, T. Shen, Z. Zhang, J. Mater. Chem., 14 (2004) 905.

Садржај: *Аморфни гвожђе (III) оксид добијен је из глине, применом амонијум хидроксида као таложног средства. Проучен је утицај методе сушења замрзавањем у вакууму на: величину честица, хемијски састав и кристаличност добијеног гвожђе (III) оксида. Након сушења замрзавањем у вакууму, добијени талог је сушен на 500 ^oC и 900 ^oC, на ваздуху. Примењене су следеће методе за карактеризацију добијених узорака: рендгенска дифракција, анализа величине честица, скенирајућа електронска микроскопија, енергетска дисперзиона спектроскопија, инфрацрвена спектроскопија са Fourier-овом трансформацијом, термограмитерија и диференцијална термијска анализа. Добијена три праха имају низак степен кристаличност, а честце непревилну слојевиту стрктуру. Код свих испитаних узорака, расподела величине пора је у уској области од око 50 μm. Добијени материјали у свом саставу садрже α- Fe_2O_3 и γ- Fe_2O_3. На кривој која је добијена диференцијалном термијском анализом, пикови који одговарају ендотермној реакцији на 620 ^oC, могу се приписати фазној трансформацији кубичне форме γ- → α- Fe_2O_3. Фазне трансформације гвожђе (III) оксида, добијеног из глине као природног извора, могу бити предмет даљих проучавања у области хемије испитивања материјала и отварају бројне могућности за синтезу материјала на бази Fe_2O_3 са специфичним магнетним особинама.*

Кључне речи: *глина; гвожђе (III) оксид; таложење; сушење замрзавањем у вакууму; ТГ; ДТА.*